Italian Journal of Food Science, 2025; 37 (1): 234–245

Red ginseng polysaccharide attenuates sepsis-induced acute lung injury via suppressing oxidative stress-mediated ER stress through activation of Nrf2/AMPK pathways

Qiuhong Liu[1], Jinqiao Zhou[2]*, Jingrui Yang[3], Xiaoqin Zhang[3], Yuna Li[1], Li Zhang[1]

[1]Department of Respiratory, the First Affiliated Hospital of Zhengzhou University, Zhengzhou, Henan, China; [2]Department of Neurosurgery, the First Affiliated Hospital of Zhengzhou University, Zhengzhou, Henan, China; [3]School of Laboratory Medicine, Xinxiang Medical University, Zhengzhou, Henan, China

*__Corresponding Author:__ Jinqiao Zhou, Department of Neurosurgery, the First Affiliated Hospital of Zhengzhou University, No. 1, Jianshe East Road, Erqi District, Henan, 450000, China. Email: zhoujinqiao0707@163.com

Academic Editor: Prof. Tommaso Beccari – Università degli Studi di Perugia, Italy

Received: 21 August 2024; Accepted: 13 September 2024; Published: 1 January 2025

ORIGINAL ARTICLE

Abstract

The present study elucidates the protective efficacy of red ginseng polysaccharide (RGP) against septic-associated acute lung injury (ALI), a critical condition exacerbated by oxidative stress and endoplasmic reticulum (ER) stress. Utilizing lipopolysaccharide (LPS)-induced mouse and cellular models, we assessed lung pathology through histological staining, injury scoring, and lung wet-to-dry ratios along with inflammatory cytokine levels. Cell viability and apoptosis were quantified using cell counting kit-8 and TUNEL assays, respectively, while fluorescence labeling was employed to gauge reactive oxygen species (ROS) and mitochondrial membrane potential (MMP). Our findings indicated that RGP markedly attenuated LPS-induced lung damage, inflammation, oxidative injury, ER stress, and apoptotic processes. Mechanistic insights revealed that RGP exerted its protective effects by activating the nuclear factor erythroid-2-related factor 2 (Nrf2)/adenosine monophosphate-activated protein kinase (AMPK) pathway in LPS-stressed lung tissues. Inhibition of Nrf2 or AMPK abrogated RGP's benefits on apoptosis, ROS production, and MMP preservation in murine lung type II epithelial (MLE-12) cells, underscoring the Nrf2/AMPK-mediated mechanism of RGP's action against LPS-induced ALI. These results underscore the potential of RGP as a novel therapeutic agent for sepsis-associated ALI.

Keywords: acute lung injury; endoplasmic reticulum stress; lipopolysaccharide; oxidative stress; red ginseng polysaccharide

Introduction

Sepsis, a condition characterized by dysregulation of host defense mechanisms, is intricately associated with organ dysfunction (Liu *et al.*, 2022a). The lungs, as the most sensitive and critical organs in sepsis, frequently succumb to acute lung injury (ALI) (Hwang *et al.*, 2019). Sepsis-induced ALI is typified by inflammatory cell infiltration, alveolar epithelium damage, pulmonary edema, and compromised gas exchange (Zhou and Liao, 2021). Emerging evidence underscores the pivotal role of excessive oxidative stress and endoplasmic reticulum (ER) stress in the pathogenesis of ALI (Guo *et al.*, 2021; Wang *et al.*, 2022a). Reactive oxygen species (ROS) are known to elicit oxidative stress within lung epithelial cells, thereby inducing ER stress and subsequent mitochondrial damage (Huang *et al.*, 2020; Yang *et al.*, 2020). Consequently, targeting the inhibition of inflammation and/or oxidative

 ISSN 1120-1770 online, DOI 10.15586/ijfs.v37i1.2760

stress-mediated ER stress emerges as a promising avenue for the prevention and treatment of sepsis-induced ALI, offering new therapeutic prospects in the management of this critical condition.

An extensive body of literature has concluded that infections caused by Gram-negative bacteria are a primary contributor to the development of ALI, with lipopolysaccharide (LPS), a key component of the bacterial outer membrane, playing a pivotal role in initiating lung injury and inflammatory responses (Fukatsu *et al.*, 2022; Li *et al.*, 2021). Exposure to LPS results in a vigorous activation of macrophages and the infiltration of inflammatory cells, notably neutrophils, into the lung (Hong *et al.*, 2022; Wang *et al.*, 2022b). This influx of neutrophils leads to the uncontrolled release of inflammatory cytokines and the generation of ROS, thereby precipitating oxidative stress (Dhlamini *et al.*, 2022; Zhou *et al.*, 2021). It is particularly intriguing that the activation or inhibition of multiple signaling pathways is closely associated with the regulation of inflammatory responses and oxidative stress in the context of LPS-induced ALI. The transcription factor nuclear factor erythroid-2-related factor 2 (*Nrf2*) is identified as a critical antioxidant regulator, and its activation is shown to prevent oxidative stress-induced cellular or tissue damage (He *et al.*, 2020). Adenosine monophosphate-activated protein kinase (AMPK), a cellular energy sensor present in various eukaryotes, also plays a role in alleviating a range of inflammatory and oxidative stress-induced diseases, including ALI (Sang *et al.*, 2022; Trefts and Shaw, 2021). Evidence suggests that activated *Nrf2* suppresses the overproduction of mitochondrial ROS and subsequently activates the AMPK signaling pathway (Chu *et al.*, 2022). Collectively, these findings underscore the potential of the Nrf2/AMPK signaling pathway to serve as a therapeutic target for attenuating ALI through its anti-inflammatory and antioxidant properties.

Medicinal herbs and their derivatives are increasingly recognized for their critical role in preventing diseases, especially those resulting from inflammation and oxidative stress, such as ALI (Yang *et al.*, 2021; Yimam *et al.*, 2023). Among these, red ginseng (RG), owing to its 'warming effect', has seen a rise in its incorporation into herbal formulas, including the famous Shenfu injection (Xu *et al.*, 2020; Zhang and Li, 2023). Previously, more research was conducted on ginsenosides and less on red ginseng polysaccharide (RGP), which is one of the active ingredients of RG (Chen *et al.*, 2019). The pharmacological potential of RGP, particularly its antitumor and antioxidant properties, has recently garnered attention (Wang *et al.*, 2023; Zhai *et al.*, 2022). Notably, RGP is shown to activate the Nrf2 pathway, enhancing antioxidant defenses and mitigating inflammatory responses, as evidenced by its efficacy in improving myocardial infarction outcomes (Lian *et al.*, 2022). However, the protective effects of RGP against septic ALI, both *in vitro* and *in vivo*, remain largely uncharted.

In this study, we aimed to elucidate the protective mechanisms of RGP on LPS-induced ALI, with a particular focus on its modulation of the Nrf2/AMPK signaling axis. Our findings provide novel insights into the therapeutic potential of RGP, offering a promising avenue for the development of innovative treatments targeting sepsis-associated ALI.

Materials and Methods

Construction of ALI model and animal grouping

Ethical approval for animal experiments was obtained from the Ethics Committee of the First Affiliated Hospital of Zhengzhou University (approval No.: 2022-03-B111). Male wild-type C57BL/6 mice, aged 6–8 weeks were randomly divided into five groups, namely, Control, LPS, LPS+dextromethorphan (DXM), LPS+RGP (200 mg/kg) and LPS+RGP (400 mg/kg). In brief, phosphate-buffered saline (PBS) solution was used to treat control animals. Mice in the LPS group were given 10 mg/kg LPS intraperitoneally (i.p.). Then, control drug dextromethorphan (DXM; D4902; Sigma-Aldrich, Shanghai, China) at a dose of 5 mg/kg or RGP (30% purity; Fufeng Sinoute Biotech Co. Ltd, Shanxi, China) at a dose of 200 mg/kg or 400 mg/kg (Lian *et al.*, 2022) was administrated intragastrically 2 h before, and 0 h and 6 h after LPS injection. Each group's 48-h survival rate was determined (10 mice per group). At 12 h after LPS challenge, the plasma and lungs were collected from the surviving mice in each group (randomly selected, 6 mice in each group). The lung tissue sections were prepared for histological analysis, fluorescence staining, Western blotting analysis and terminal deoxynucleotidyl transferase-mediated dUTP nick-end labeling (TUNEL) apoptosis assay. The plasma samples were applied for enzyme-linked immunosorbent serological assay (ELISA).

Cell treatment

ALI cellular model was constructed by continuous stimulation of murine lung type II epithelial (MLE-12) cell line (CRL-2110™; ATCC, Manassas, VA, USA), a mouse lung epithelial cell line, for 24 h with LPS (L4516; Sigma-Aldrich) at a final concentration of 500 ng/mL (Liu *et al.*, 2022b; Xiao *et al.*, 2020). In certain groups, MLE-12 cells were pretreated with *Nrf2* inhibitor ML385 (20 μM; SML1833; Sigma-Aldrich) for 2 h or AMPK inhibitor Compound C (10 μM; 171260; Sigma-Aldrich) for 1 h,

and then co-incubated with 40-μg/mL RGP for 24 h prior to LPS stimulation.

Histological analysis

Lung tissues were fixed in 10% formalin for 24 h, embedded in paraffin, and cut into 5-μm thick sections for hematoxylin and eosin (H&E) staining. Histopathological changes were observed under a light microscope (Olympus Corporation, Tokyo, Japan), and the severity of lung injury was assessed using a semi-quantitative scale (He *et al.*, 2022; Li *et al.*, 2015).

Analysis of wet-to-dry ratio of lungs

The collected lung tissues were blotted and weighed to obtain wet weight and then dried in an oven at 80°C for 48 h to obtain dry weight. The wet-to-dry ratio of the lungs was calculated to assess the degree of pulmonary edema.

ELISA assays

Using mouse ELISA kits (Beyotime Biotechnology, Shanghai, China), the protein levels of tumor necrosis factor-α (TNF-α), interleukin-1β (IL-1β), and IL-6 were determined in plasma samples, according to the manufacturer's instructions.

Measurement of reactive oxygen species generation

The production of ROS in tissues and cells was measured with the fluorescent probe 2',7'-dichlorofluorescein diacetate (DCF-DA) using ROS assay kit (S0033S; Beyotime Biotechnology). Lung tissue homogenate supernatants and rinsed MLE-12 cells were incubated with 10-μM DCF-DA for 20 min at 37°C in the dark. Samples were photographed using a fluorescent microscope (Zeiss, New York, NY, USA).

Quantitative real time polymerase chain reaction (qRT-PCR)

Total RNA was isolated from tissues using the TRIzol™ reagent (Invitrogen, Waltham, MA, USA). PrimeScript™ RealTime (RT) reagent kit (Takara, Japan) was used to create complementary DNA (cDNA). qRT-PCR was performed on the Light Cycler 480 II RT-PCR system (Roche, Basel, Switzerland) using SYBR Premix Ex Taq II (TaKaRa, Shiga, Japan). The $2^{-\Delta\Delta Ct}$ method was used to calculate relative RNA abundance. The expression level of glyceraldehyde 3-phosphate dehydrogenase (GAPDH) was taken as a negative control. The following primers were used in this study: Bcl-2-associated X-protein (Bax): 5'-AGACAGGGGCCTTTTTGCTAC-3' (forward), 5'-AATTCGCCGGAGACACTCG-3' (reverse); B-cell lymphoma 2 (Bcl-2): 5'-GTCGCTACCGTCG TGACTTC-3' (forward), 5'-CAGACATGCACCTACC CAGC-3' (reverse); and GAPDH: 5'-AGGTCGGTGTGA ACGGATTTG-3' (forward), 5'-GGGGTCGTTGATGG CAACA-3' (reverse).

Western blot analysis

Lung tissues were homogenized and lysed using radioimmunoprecipitation assay (RIPA; Thermo Scientific, Shanghai, China), and the lysate was centrifuged at 12,000 ×*g* for 5 min at 4°C. The supernatant was stored at –20°C. The contents of target proteins were determined according to the bicinchoninic acid assay (BCA), and separated by electrophoresis. After transferring to nitrocellulose membranes (Millipore, Bedford, MA, USA), proteins were hybridized with primary antibodies overnight at 4°C and secondary antibodies (1:2,000 dilution; #7074; Cell Signaling Technology, Boston, MA, USA) for 2 h at room temperature. Immunodetection was performed using the enhanced chemiluminescence reagent (Beckman Coulter, Brea, CA, USA).

TUNEL assays

Apoptosis in lung tissues was analyzed by TUNEL staining using One Step TUNEL apoptosis assay kit (C1086; Beyotime Biotechnology). Images were obtained using a microscope.

Cell viability assay

Cell viability was determined using Cell Counting Kit-8 assay (CCK-8) (C0037; Beyotime Biotechnology). Following different treatments, MLE-12 cells with a molecular mass of 100 μL were incubated in 96-well plates at a density of 2,000/well. Absorbance was detected at the wavelength of 450 nm after the addition of 10-μL CCK-8 solution.

Flow cytometry (FCM)

The Annexin V-FITC apoptosis detection kit (C1062S; Beyotime Biotechnology) was used to evaluate apoptotic cells according to the manufacturer's instructions. MLE-12 cells were washed with PBS, resuspended in 1× binding buffer, and stained with 5-μL Annexin V-FITC for 10 min. The cells were analyzed using a flow cytometer (BD Biosciences, San Diego, CA, USA) after counterstained with 10-μL propidium iodide (PI) for 10 min.

Detection of mitochondrial membrane potential (MMP)

The MMP was detected using MMP assay kit with JC-1 staining working solution (C2006; Beyotime Biotechnology). Briefly, MLE-12 cells (1×10^5 cells resuspended in 500-μL cell culture medium) were incubated for 20 min at 37°C with 0.5-mL JC-1. After centrifugation at 600 ×*g* for 3 min at 4°C, the supernatant was discarded. After washing twice with JC-1 staining buffer, cells were resuspended in JC-1 staining buffer and observed with fluorescence microscopy.

Statistical analysis

Data were presented as mean ± standard deviation (SD). GraphPad Prism 6.0 (GraphPad Software, San Diego, CA, USA) was used for data analysis using ANOVA, followed by Tukey's test; $p < 0.05$ was considered as statistically significant.

Results

Red ginseng polysaccharide ameliorates LPS-induced lung injury and inflammation in mice

To ascertain the protective efficacy of RGP against sepsis-associated ALI, we established a mouse model of LPS-induced ALI. Initially, we monitored the survival rate over 48 h post-LPS challenge, revealing that treatment with 400-mg/kg RGP conferred a protective effect on mouse survival against LPS-induced effects, akin to the positive control drug dextromethorphan (DXM; Figure 1A). Histopathological alterations in each group of mice were further examined via H&E staining. Inflammatory cell infiltration, interstitial edema, alveolar wall thickening, and tissue damage were commonly observed in LPS-induced mice; both DXM intervention and 400-mg/kg RGP markedly alleviated the pulmonary injury induced by LPS (Figure 1B), which was also quantified using lung injury scores (Figure 1C). Subsequently, we assessed the impact of RGP on LPS-induced pulmonary edema. As depicted in Figure 1D, the lung wet-to-dry weight ratio was significantly elevated in the LPS group, compared to the control group, an increase that was mitigated by treatment with either DXM or RGP. To investigate the effect of RGP on LPS-induced inflammatory responses, we measured the expression of pro-inflammatory cytokines, including TNF-α, IL-1β, and IL-6, in plasma via ELISA. As illustrated in Figure 1E, LPS administration resulted in substantial elevations in the plasma levels of these cytokines, which were reversed by either DXM or RGP. The anti-inflammatory action of RGP underscored its potential as a functional food ingredient, offering promise in mitigating inflammation-related diseases, including sepsis-induced ALI.

Red ginseng polysaccharide suppresses oxidative stress and ER stress in LPS-induced mouse lung tissues

The assessment of DCF-DA fluorescence intensity revealed that pretreatment with DXM or RGP markedly attenuated the LPS-induced overproduction of ROS, as evidenced in Figure 2A. LPS administration led to the up-regulation of glucose-regulated protein 78 (GRP78) and C/EBP homologous protein (CHOP), as well as the activation of protein kinase RNA-like endoplasmic reticulum kinase (PERK) in mouse lung tissues, accompanied by increased phosphorylation levels of eukaryotic initiation factor 2 alpha (eIF2α), PERK, and inositol requiring protein-1α (IRE1α). Notably, these LPS-induced alterations were significantly mitigated by pretreatment with DXM or RGP, as depicted in Figures 2B and 2C. Collectively, these findings suggested that RGP has the potential to prevent oxidative stress and ER stress, thereby alleviating LPS-induced ALI.

Red ginseng polysaccharide inhibits LPS-induced lung cell apoptosis in LPS-challenged mice

The level of apoptosis was subsequently evaluated using TUNEL labeling to delineate the impact of RGP on LPS-induced apoptosis within the pulmonary tissues of mice. Quantitative analysis of apoptotic cells indicated a notably higher count in the LPS-treated group whereas a pronounced decrease in apoptotic cells was observed following treatment with DXM or RGP (Figure 3A). The results of qRT-PCR and Western blot analyses demonstrated that both DXM and RGP effectively mitigated the LPS-induced elevation of Bax messenger RNA (mRNA) and protein levels, along with the corresponding decrease in Bcl-2 expression (Figures 3B and 3C). Collectively, these results suggested that RGP intervention could efficaciously inhibit LPS-induced apoptosis in lung tissue cells, underscoring its potential therapeutic implications in mitigating lung injury.

Red ginseng polysaccharide activates Nrf2/AMPK signaling pathway in LPS-induced ALI mice

Further analysis was conducted to evaluate the activities of Nrf2 and AMPK, molecular pathways known to mitigate lung injury (Qiu *et al.*, 2018; Yang *et al.*, 2022) using Western blot analysis (Figures 4A and 4B). Our findings indicated that LPS exposure resulted in a slight, albeit nonsignificant, increase in *Nrf2* expression and a significant decrease in AMPK phosphorylation within lung

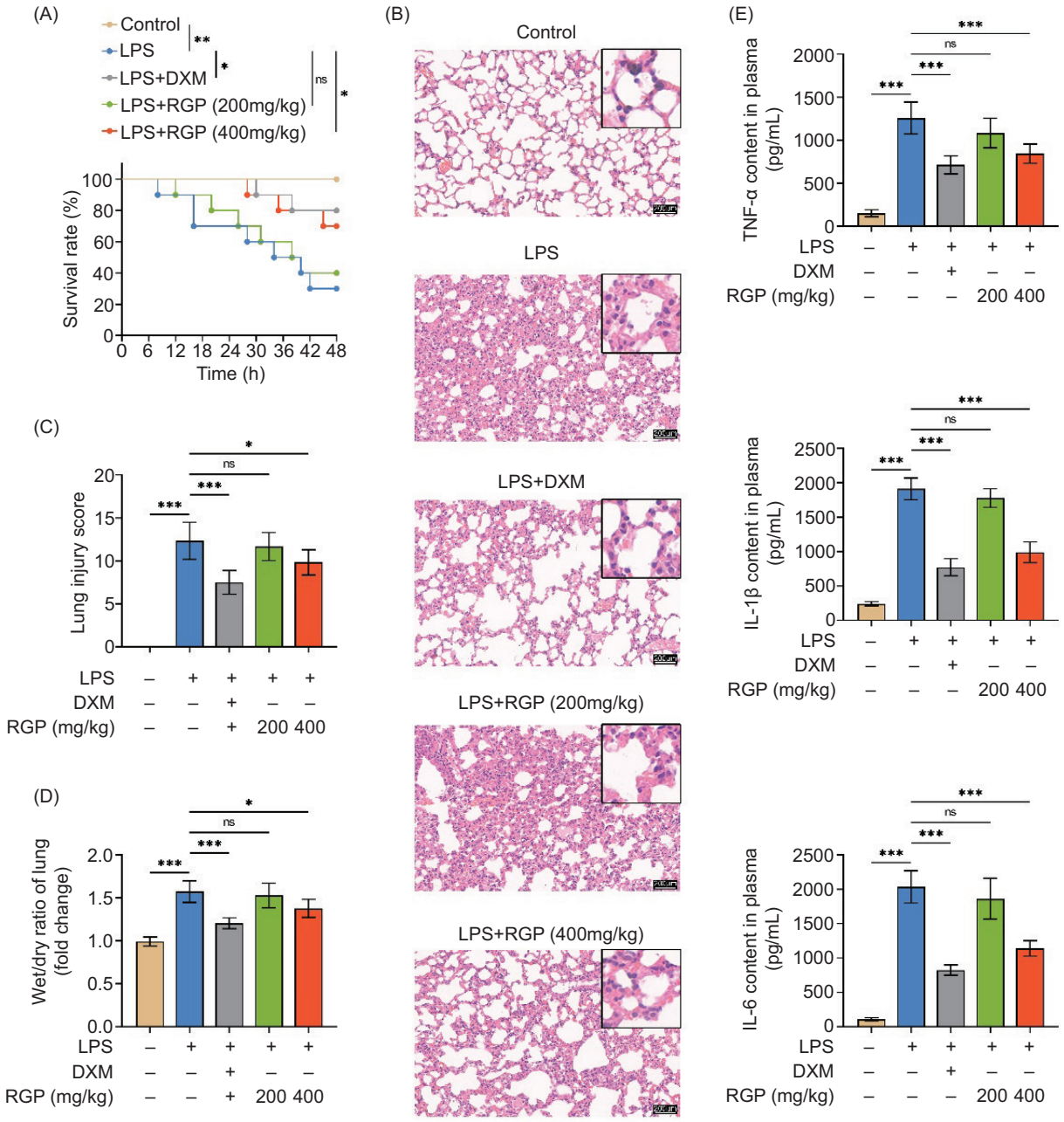

Figure 1. RGP ameliorates LPS-induced lung injury and inflammation in mice. LPS (10 mg/kg) was intraperitoneally administrated to induce ALI; 2 h before and 0 h and 6 h after LPS challenge, DXM (5 mg/kg) or RGP (200 mg/kg or 400 mg/kg) was given to each administration group. (A) Survival curves of five groups (n = 10). (B) H & E staining of lung tissues from each group of mice (scale bar: 200 μm; n = 6). (C) The lung injury score was calculated by a semi-quantitative scale in different groups (n = 6). (D) The lung wet-to-dry weight ratio (n = 6). (E) Levels of TNF-α, IL-1β, and IL-6 in plasma were determined by ELISA (n = 6). Results are presented as mean ± SD obtained from six independent experiments; *$p < 0.05$; ***$p < 0.001$.

tissues. However, pretreatment with DXM or RGP led to the up-regulation of *Nrf2* and a marked enhancement of AMPK phosphorylation in LPS-challenged mice. These results suggested that both DXM and RGP are capable of effectively activating the Nrf2/AMPK signaling pathway, which plays a pivotal role in conferring protection against LPS-induced ALI.

Red ginseng polysaccharide ameliorates LPS-induced injury in MLE-12 cells by activating the Nrf2/AMPK pathway

Based on the above *in vivo* findings, we proceeded to explore the potential of RGP to mitigate LPS-induced cellular injury in MLE-12 cells. CCK-8 assays revealed that

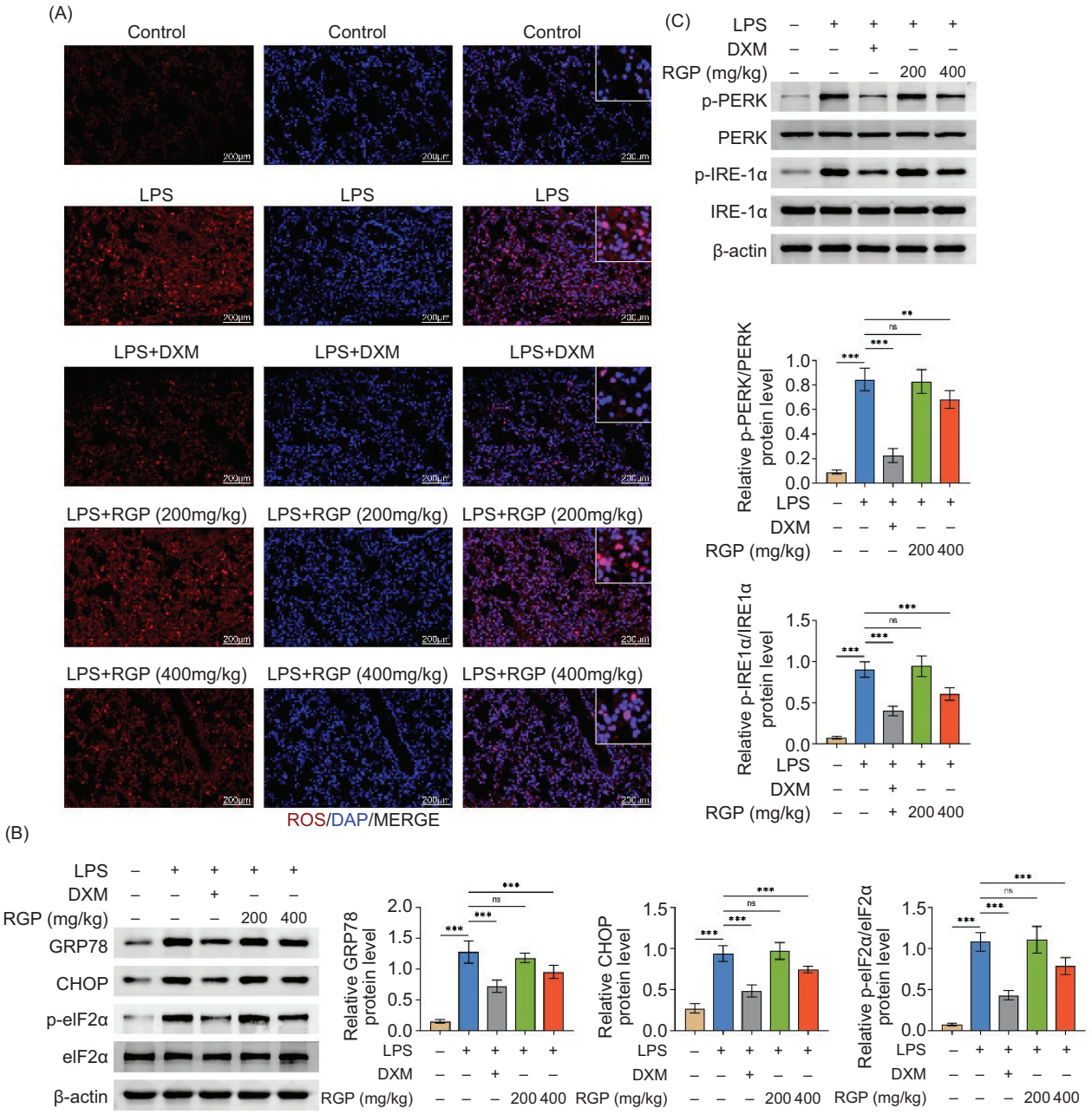

Figure 2. RGP suppresses LPS-induced oxidative stress and ER stress in mouse lung tissues. (A) The fluorescence images of ROS production stained by DCF-DA (scale bar: 200 μm). (B) The protein levels of GRP78, CHOP, p-eIF2α, and total eIF2α were determined in lung tissues of different groups. (C) The phosphorylation and total levels of PERK and IRE1α were determined in lung tissues of different groups. Results are presented as mean ± SD (n = 6) obtained from six independent experiments; **$p < 0.01$; ***$p < 0.001$.

RGP at concentrations of 10, 20, and 40 μg/mL exhibited no cytotoxic effects, with significant cytotoxicity only observed at 80 μg/mL (Figure 5A). Following LPS stimulation, cell viability was notably diminished; however, treatment with RGP at 20 μg/mL or 40 μg/mL significantly attenuated the LPS-induced decline in cell viability (Figure 5B). Consequently, we selected a concentration of 40 μg/mL RGP for subsequent experiments. To elucidate the involvement of the Nrf2/AMPK signaling pathway in RGP's mechanism of action, cells were co-treated with ML385 (an inhibitor of *Nrf2*) or Compound C (an inhibitor of AMPK). In alignment with the *in vivo* findings, RGP demonstrated inhibition of LPS-induced cell death in MLE-12 cells whereas co-administration with ML385 or Compound C notably counteracted the anti-apoptotic effects of RGP (Figure 5C). Mitochondria are widely considered the primary site of ROS formation, and MMP is an important parameter reflecting mitochondrial function

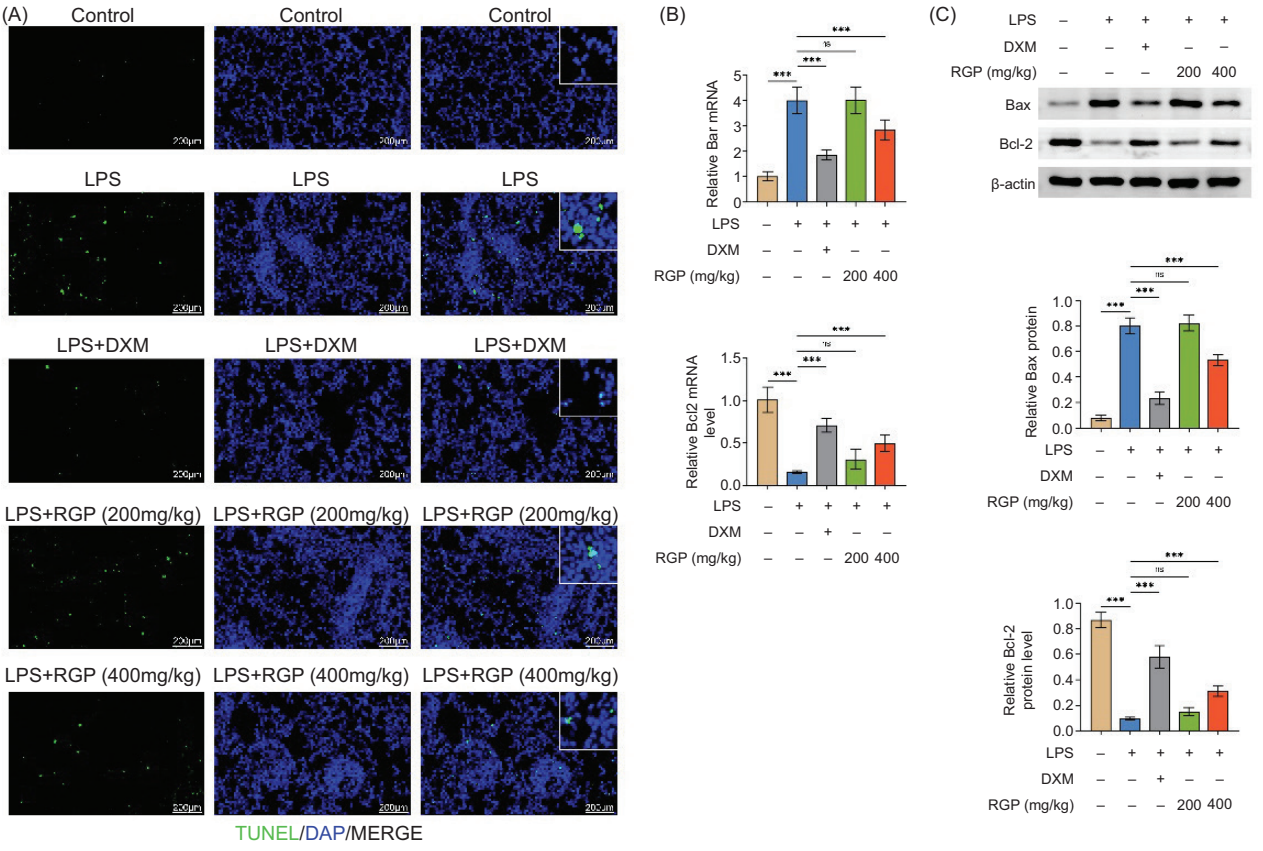

Figure 3. RGP inhibits LPS-induced lung cell apoptosis in LPS-challenged mice. (A) The apoptosis of lung tissue cells was detected by TUNEL assay (scale bar: 200 μm). (B) The mRNA expressions of Bax and Bcl-2 in lung tissues of different groups were determined by qRT-PCR. (C) The protein levels of Bax and Bcl-2 in lung tissues of different groups were determined by Western blot analysis. Results are presented as mean ± SD (n = 6) obtained from six independent experiments; ***$p < 0.001$.

(Correia-Álvarez *et al.*, 2020; Rehfeldt *et al.*, 2021). In this study, LPS markedly induced ROS production and a reduction in MMP within MLE-12 cells, indicative of oxidative stress injury and mitochondrial dysfunction. On the contrary, RGP protected MLE-12 cells from LPS-induced ROS overproduction (Figure 5D) and MMP reduction (Figures 5E and 5F), and its protective effects were restored by the inhibitors of Nrf2 and AMPK.

Discussion

Sepsis-induced ALI is a complex hypoxic condition characterized by multifaceted pathological mechanisms, including apoptosis, inflammation, oxidative stress, and ER stress (Chen *et al.*, 2018; Qian *et al.*, 2020; Zeng *et al.*, 2017). RGP, a principal bioactive component of RG, has demonstrated tumor-suppressive (Zhai *et al.*, 2022) and antioxidant properties (Kang *et al.*, 2023; Lian *et al.*, 2022). The current study identified RGP as a promising therapeutic agent for alleviating sepsis-associated ALI, suggesting that its protective effects against LPS-induced ALI may be mediated through the activation of the Nrf2/AMPK signaling pathway.

Extensive evidence is observed that LPS could act as a cytotoxic agent capable of inducing ALI both *in vivo* and *in vitro*, leading to pathological damage, apoptosis, and inflammation (Li *et al.*, 2023a, 2023b). In this study, RGP exhibited therapeutic effects comparable to the positive control drug DXM in LPS-induced ALI mice. This was evidenced by enhanced survival proportions, diminished pulmonary pathological lesions, lower lung injury scores and wet-to-dry ratios, and reduced plasma pro-inflammatory cytokine levels. In addition, RGP demonstrated an inhibitory effect on apoptosis within the lung tissues of mice with sepsis-induced ALI.

Endoplasmic reticulum stress arises from the accumulation of unfolded or misfolded proteins, leading to a disruption in ER's structural and functional equilibrium (Dandekar *et al.*, 2015; Schwarz and Blower, 2016). This stress is a critical pathogenic mechanism in sepsis-associated ALI and holds potential as a biomarker and

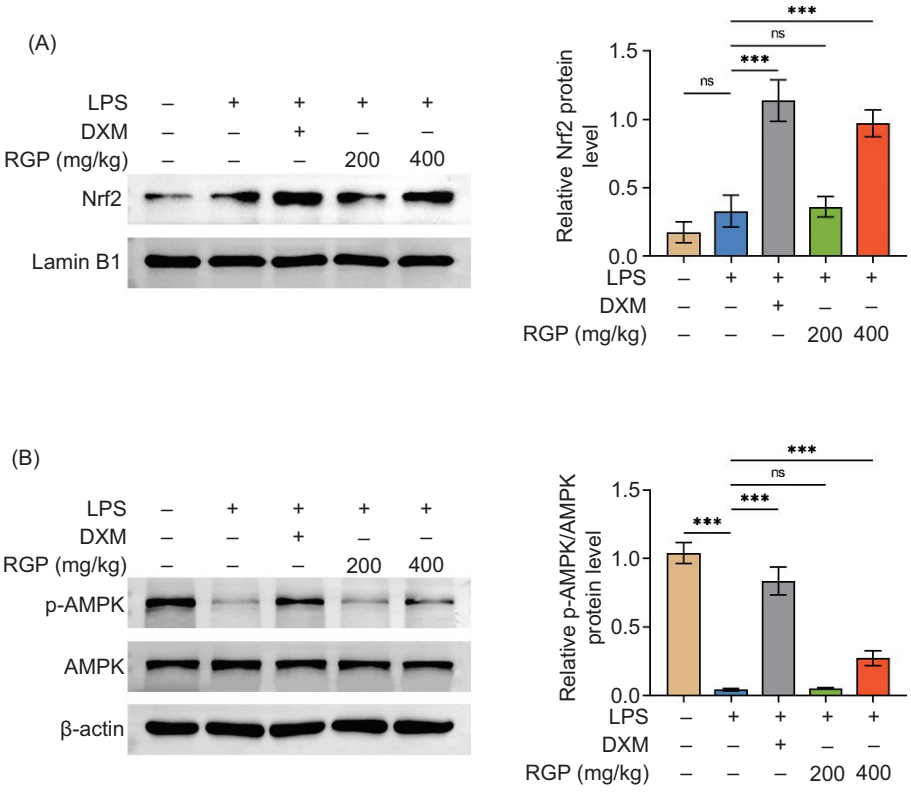

Figure 4. RGP activates Nrf2/AMPK signaling pathway in LPS-induced ALI mice. (A) The protein levels of Nrf2 were determined in lung tissues of different groups. (B) The protein levels of p-AMPK and total AMPK were determined in lung tissues of different groups. Results are presented as mean ± SD (n = 6) obtained from six independent experiments; ***$p < 0.001$.

therapeutic target for sepsis (Ahmad *et al.*, 2022; Zeng *et al.*, 2023). In a mouse model of LPS-induced ALI, pretreatment with RGP ameliorated lung oxidative damage by reducing ROS production and mitigated ER stress by down-regulating ER stress markers GRP78 and CHOP (Arab *et al.*, 2023) and decreasing phosphorylation levels of the unfolded protein response (UPR) sensors eIF2α, PERK, and IRE1α (Men *et al.*, 2023). In LPS-stimulated MLE-12 cells, RGP exhibited anti-apoptotic effects and enhanced mitochondrial function, evidenced by decreased ROS release and increased MMP, suggesting a protective role against LPS-induced ALI through anti-apoptotic, anti-inflammatory, and anti-stress mechanisms. Further studies are warranted to fully elucidate this hypothesis.

To further elucidate the protective mechanism of RGP, we examined its influence on the Nrf2/AMPK pathway. *Nrf2*, a redox-sensitive transcriptional regulator, orchestrates the expression of antioxidant genes to maintain cellular redox balance and mitigate ER stress (Huang *et al.*, 2020). AMPK plays a pivotal role in modulating energy metabolism and mitochondrial biogenesis in response to energy deficits (Sang *et al.*, 2022; Tang *et al.*, 2022).

Accumulating evidence suggests that various herbal bioactive components confer protection against ALI by activating the Nrf2/AMPK signaling pathway. For instance, Lv *et al.* (2017) reported that xanthohumol effectively protected LPS-induced ALI against oxidative stress and inflammation damage, which are largely dependent upon up-regulation of the Nrf2 pathway via activation of AMPK/GSK3β. Lycium barbarum polysaccharide (LBP) ameliorated lung inflammation and edema in a mouse model of hyperoxia-induced ALI through an Nrf2/AMPK-dependent mechanism (Zheng *et al.*, 2019). Sophoricoside exhibited anti-inflammatory effects in LPS-induced ALI mice and macrophages via Nrf2/AMPK signaling (Wu *et al.*, 2021). Kinsenoside prevented LPS-induced ALI by activating Nrf2/AMPK and regulating mitochondrial function (Yang *et al.*, 2022). In our study, RGP up-regulated *Nrf2* expression and induced AMPK phosphorylation in LPS-induced ALI mice. Furthermore, the inhibition of Nrf2/AMPK signaling in MLE-12 cells with ML385 and compound C partially negated RGP's anti-apoptotic, antioxidant, and anti-ER stress effects in LPS-treated cells.

The current study, however, has limitations. First, the genomic differences between mice and humans (Lewis *et al.*, 2016) in response to sepsis necessitate validation

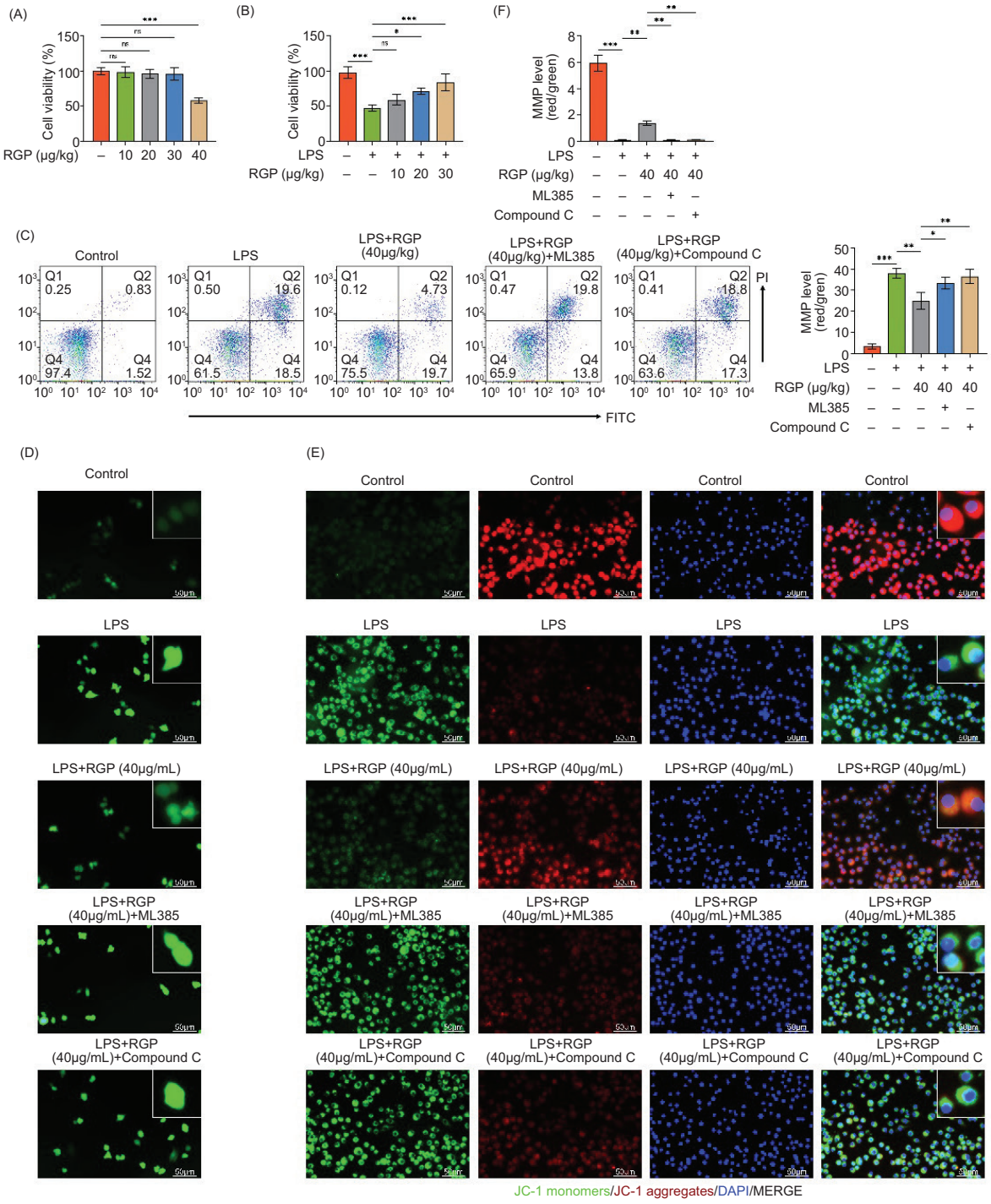

Figure 5. RGP ameliorates LPS-induced injury in MLE-12 cells by activating the Nrf2/AMPK pathway. MLE-12 cells were treated with different concentrations of RGP (0, 10, 20, 40, and 80 μg/mL), and the cell viability was evaluated by CCK-8 assay. (A) MLE-12 cells were treated with different concentrations of RGP (0, 10, 20, and 40 μg/mL) in the presence of LPS (500 ng/mL) for 24 h, and the cell viability was evaluated by CCK-8 assay. (B) MLE-12 cells were treated with RGP (40 μg/mL) or co-treated with ML385 or Compound C in the presence of LPS (500 ng/mL) for 24 h; then cells were collected and used for apoptosis, oxidative stress, and ER stress detection. (C) Apoptosis rate was analyzed by FCM. (D) The intracellular ROS production was assessed by DCF-DA fluorescence staining. (E) JC-1 staining results: green represents MMP monomers and red represents MMP aggregate. (F) Representative histograms depicting MMP levels. Results are presented as mean ± SD (n = 3) obtained from three independent experiments; *$p < 0.05$, **$p < 0.01$, and ***$p < 0.001$.

of these findings in murine models of cecal ligation and puncture (CLP). In addition, the complex pathophysiology of ALI involves multiple signaling pathways, warranting further research to achieve a comprehensive understanding of the underlying mechanisms. Further studies are required to delineate the regulatory role of RGP on the Nrf2/AMPK signaling pathway.

Conclusions

The present study demonstrates that RGP, a key component of RG, protects against sepsis-induced ALI by modulating the Nrf2/AMPK pathway. These findings highlight the potential of RGP as a functional food ingredient with therapeutic applications in managing sepsis-related complications, thereby contributing to the growing field of nutraceuticals to enhance immune and respiratory health through diet.

Availability of Data and Materials

All data generated or analyzed in this study are included in this published article. The datasets used and/or analyzed in the present study are available from the corresponding author on reasonable request.

Author Contributions

Qiuhong Liu and Jinqiao Zhou designed the study, completed the experiment, and supervised data collection. Jingrui Yang analyzed and interpreted the data. Xiaoqin Zhang, Yuna Li, and Li Zhang prepared the manuscript for publication and reviewed draft of the manuscript. All authors read and approved the final manuscript.

Conflict of Interest

None.

Funding and Competing Interests

This work was supported by the Henan Province Medical Science and Technology Key Project, jointly constructed by the Provincial and Ministerial Departments (Grant No. SBGJ202102172). The authors stated that there was no conflict of interest to disclose.

References

Ahmad S., Zaki A., Manda K., Mohan A. and Syed M.A. 2022. Vitamin-D ameliorates sepsis-induced acute lung injury via augmenting miR-149-5p and down-regulating ER stress. J Nutr Biochem. 110:109130. https://doi.org/10.1016/j.jnutbio.2022.109130

Arab H.H., Khames A., Alsufyani S.E., El-Sheikh A.A.K. and Gad A.M. 2023. Targeting the endoplasmic reticulum stress-linked PERK/GRP78/CHOP pathway with magnesium sulfate attenuates chronic-restraint-stress-induced depression-like neuropathology in rats. Pharmaceuticals (Basel). 16(2):300. https://doi.org/10.3390/ph16020300

Chen J., Li M., Qu D. and Sun Y. 2019. Neuroprotective effects of red ginseng saponins in scopolamine-treated rats and activity screening based on pharmacokinetics. Molecules. 24(11):2136. https://doi.org/10.3390/molecules24112136

Chen X., Wang Y., Xie X., Chen H., Zhu Q., Ge Z., *et al.* 2018. Heme oxygenase-1 reduces sepsis-induced endoplasmic reticulum stress and acute lung injury. Mediators Inflamm. 2018:9413876. https://doi.org/10.1155/2018/9413876

Chu X., Li L., Yan W. and Ma H. 2022. 4-Octyl itaconate prevents free fatty acid-induced lipid metabolism disorder through activating Nrf2-AMPK signaling pathway in hepatocytes. Oxid Med Cell Longev. 2022:5180242. https://doi.org/10.1155/2022/5180242

Correia-Álvarez E., Keating J.E., Glish G., Tarran R. and Sassano M.F. 2020. Reactive oxygen species, mitochondrial membrane potential, and cellular membrane potential are predictors of E-liquid-induced cellular toxicity. Nicotine Tob Res. 22(Suppl 1):S4–S13. https://doi.org/10.1093/ntr/ntaa177

Dandekar A., Mendez R. and Zhang K. 2015. Cross talk between ER stress, oxidative stress, and inflammation in health and disease. Methods Mol Biol. 1292:205–214. https://doi.org/10.1007/978-1-4939-2522-3_15

Dhlamini Q., Wang W., Feng G., Chen A., Chong L., Li X., *et al.* 2022. FGF1 alleviates LPS-induced acute lung injury via suppression of inflammation and oxidative stress. Mol Med. 28(1):73. https://doi.org/10.1186/s10020-022-00502-8

Fukatsu M., Ohkawara H., Wang X., Alkebsi L., Furukawa M., Mori H., *et al.* 2022. The suppressive effects of Mer inhibition on inflammatory responses in the pathogenesis of LPS-induced ALI/ARDS. Sci Signal. 15(724):eabd2533. https://doi.org/10.1126/scisignal.abd2533

Guo Y., Liu Y., Zhao S., Xu W., Li Y., Zhao P., *et al.* 2021. Oxidative stress-induced FABP5 S-glutathionylation protects against acute lung injury by suppressing inflammation in macrophages. Nat Commun. 12(1):7094. https://doi.org/10.1038/s41467-021-27428-9

He R., Liu B., Xiong R., Geng B., Meng H., Lin W., *et al.* 2022. Itaconate inhibits ferroptosis of macrophage via Nrf2 pathways against sepsis-induced acute lung injury. Cell Death Discov. 8(1):43. https://doi.org/10.1038/s41420-021-00807-3

He F., Ru X. and Wen T. 2020. Nrf2, a transcription factor for stress response and beyond. Int J Mol Sci. 21(13):4777. https://doi.org/10.3390/ijms21134777

Hong H., Lou S., Zheng F., Gao H., Wang N., Tian S., *et al.* 2022. Hydnocarpin D attenuates lipopolysaccharide-induced acute lung injury via MAPK/NF-κB and Keap1/Nrf2/HO-1 pathway. Phytomedicine. 101:154143. https://doi.org/10.1016/j.phymed.2022.154143

Huang C.Y., Deng J.S., Huang W.C., Jiang W.P. and Huang G.J. 2020. Attenuation of lipopolysaccharide-induced acute lung injury by hispolon in mice, through regulating the TLR4/PI3K/Akt/mTOR and Keap1/Nrf2/HO-1 pathways, and suppressing oxidative stress-mediated ER stress-induced apoptosis and autophagy. Nutrients. 12(6):1742. https://doi.org/10.3390/nu12061742

Hwang J.S., Kim K.H., Park J., Kim S.M., Cho H., Lee Y., et al. 2019. Glucosamine improves survival in a mouse model of sepsis and attenuates sepsis-induced lung injury and inflammation. J Biol Chem. 294(2):608–622. https://doi.org/10.1074/jbc.RA118.004638

Kang J., Zhao J., He L.F., Li L.X., Zhu Z.K. and Tian M.L. 2023. Extraction, characterization and anti-oxidant activity of polysaccharide from red Panax ginseng and Ophiopogon japonicus waste. Front Nutr. 10:1183096. https://doi.org/10.3389/fnut.2023.1183096

Lewis A.J., Seymour C.W. and Rosengart M.R. 2016. Current murine models of sepsis. Surg Infect (Larchmt). 17(4):385–393. https://doi.org/10.1089/sur.2016.021

Li G., Hu C., Liu Y. and Lin H. 2023a. Ligustilide, a novel SIRT1 agonist, alleviates lipopolysaccharide-induced acute lung injury through deacetylation of NICD. Int Immunopharmacol. 121:110486. https://doi.org/10.1016/j.intimp.2023.110486

Li J., Lu K., Sun F., Tan S., Zhang X., Sheng W., *et al.* 2021. Panaxydol attenuates ferroptosis against LPS-induced acute lung injury in mice by Keap1-Nrf2/HO-1 pathway. J Transl Med. 19(1):96. https://doi.org/10.1186/s12967-021-02745-1

Li Y., Xiao W. and Lin X. 2023b. Long noncoding RNA MALAT1 inhibition attenuates sepsis-induced acute lung injury through modulating the miR-129-5p/PAX6/ZEB2 axis. Microbiol Immunol. 67(3):142–153. https://doi.org/10.1111/1348-0421.13045

Li B., Zeng M., He W., Huang X., Luo L., Zhang H., *et al.* 2015. Ghrelin protects alveolar macrophages against lipopolysaccharide-induced apoptosis through growth hormone secretagogue receptor 1a-dependent c-Jun N-terminal kinase and Wnt/beta-catenin signaling and suppresses lung inflammation. Endocrinology. 156(1):203–217. https://doi.org/10.1210/en.2014-1539

Lian Y., Zhu M., Yang B., Wang X., Zeng J., Yang Y., *et al.* 2022. Characterization of a novel polysaccharide from red ginseng and its ameliorative effect on oxidative stress injury in myocardial ischemia. Chin Med. 17(1):111. https://doi.org/10.1186/s13020-022-00669-6

Liu D., Huang S.Y., Sun J.H., Zhang H.C., Cai Q.L., Gao C., *et al.* 2022a. Sepsis-induced immunosuppression: mechanisms, diagnosis and current treatment options. Mil Med Res. 9(1):56. https://doi.org/10.1186/s40779-022-00422-y

Liu J., Yao S., Jia J., Chen Z., Yuan Y., He Y., *et al.* 2022b. Loss of MBD2 ameliorates LPS-induced alveolar epithelial cell apoptosis and ALI in mice via modulating intracellular zinc homeostasis. FASEB J. 36(2):e22162. https://doi.org/10.1096/fj.202100924RR

Lv H., Liu Q., Wen Z., Feng H., Deng X. and Ci X. 2017. Xanthohumol ameliorates lipopolysaccharide (LPS)-induced acute lung injury via induction of AMPK/GSK3β-Nrf2 signal axis. Redox Biol. 12:311–324. https://doi.org/10.1016/j.redox.2017.03.001

Men L., Guo J., Cao Y., Huang B., Wang Q., Huo S., *et al.* 2023. IL-6/GP130/STAT3 signaling contributed to the activation of the PERK arm of the unfolded protein response in response to chronic beta-adrenergic stimulation. Free Radic Biol Med. 205:163–174. https://doi.org/10.1016/j.freeradbiomed.2023.06.005

Qian Q., Cao X., Wang B., Dong X., Pei J., Xue L., *et al.* 2020. Endoplasmic reticulum stress potentiates the autophagy of alveolar macrophage to attenuate acute lung injury and airway inflammation. Cell Cycle. 19(5):567–576. https://doi.org/10.1080/15384101.2020.1718851

Qiu Y.L., Cheng X.N., Bai F., Fang L.Y., Hu H.Z. and Sun D.Q. 2018. Aucubin protects against lipopolysaccharide-induced acute pulmonary injury through regulating Nrf2 and AMPK pathways. Biomed Pharmacother. 106:192–199. https://doi.org/10.1016/j.biopha.2018.05.070

Rehfeldt S.C.H., Laufer S. and Goettert M.I. 2021. A highly selective *in vitro* JNK3 inhibitor, FMU200, restores mitochondrial membrane potential and reduces oxidative stress and apoptosis in SH-SY5Y cells. Int J Mol Sci. 22(7):3701. https://doi.org/10.3390/ijms22073701

Sang A., Wang Y., Wang S., Wang Q., Wang X., Li X., *et al.* 2022. Quercetin attenuates sepsis-induced acute lung injury via suppressing oxidative stress-mediated ER stress through activation of SIRT1/AMPK pathways. Cell Signal. 96:110363. https://doi.org/10.1016/j.cellsig.2022.110363

Schwarz D.S. and Blower M.D. 2016. The endoplasmic reticulum: structure, function and response to cellular signaling. Cell Mol Life Sci (CMLS). 73(1):79–94. https://doi.org/10.1007/s00018-015-2052-6

Tang Y., Wa Q., Peng L., Zheng Y., Chen J., Chen X., *et al.* 2022. Salvianolic acid B suppresses ER stress-induced NLRP3 inflammasome and pyroptosis via the AMPK/FoxO4 and syndecan-4/Rac1 signaling pathways in human endothelial progenitor cells. Oxid Med Cell Longev. 2022:8332825. https://doi.org/10.1155/2022/8332825

Trefts E. and Shaw R.J. 2021. AMPK: restoring metabolic homeostasis over space and time. Mol Cell. 81(18):3677–3690. https://doi.org/10.1016/j.molcel.2021.08.015

Wang F., Ma J., Wang J., Chen M., Xia H., Yao S., *et al.* 2022a. SIRT1 ameliorated septic associated-lung injury and macrophages apoptosis via inhibiting endoplasmic reticulum stress. Cell Signal. 97:110398. https://doi.org/10.1016/j.cellsig.2022.110398

Wang Y., Wang X., Li Y., Xue Z., Shao R., Li L., *et al.* 2022b. Xuanfei Baidu decoction reduces acute lung injury by regulating infiltration of neutrophils and macrophages via PD-1/IL17A pathway. Pharmacol Res. 176:106083. https://doi.org/10.1016/j.phrs.2022.106083

Wang S., Zhao Y., Yang J., Liu S., Ni W., Bai X., *et al.* 2023. Ginseng polysaccharide attenuates red blood cells oxidative stress injury by regulating red blood cells glycolysis and liver gluconeogenesis. J Ethnopharmacol. 300:115716. https://doi.org/10.1016/j.jep.2022.115716

Wu Y.X., Zeng S., Wan B.B., Wang Y.Y., Sun H.X., Liu G., *et al.* 2021. Sophoricoside attenuates lipopolysaccharide-induced acute lung injury by activating the AMPK/Nrf2 signaling axis.

Int Immunopharmacol. 90:107187. https://doi.org/10.1016/j.intimp.2020.107187

Xiao K., He W., Guan W., Hou F., Yan P., Xu J., *et al.* 2020. Mesenchymal stem cells reverse EMT process through blocking the activation of NF-kappaB and hedgehog pathways in LPS-induced acute lung injury. Cell Death Dis. 11(10):863. https://doi.org/10.1038/s41419-020-03034-3

Xu P., Zhang W.Q., Xie J., Wen Y.S., Zhang G.X. and Lu S.Q. 2020. Shenfu injection prevents sepsis-induced myocardial injury by inhibiting mitochondrial apoptosis. J Ethnopharmacol. 261:113068. https://doi.org/10.1016/j.jep.2020.113068

Yang H., Song Z. and Hong D. 2020. CRBN knockdown mitigates lipopolysaccharide-induced acute lung injury by suppression of oxidative stress and endoplasmic reticulum (ER) stress associated NF-kappaB signaling. Biomed Pharmacother. 123:109761. https://doi.org/10.1016/j.biopha.2019.109761

Yang R., Yang H., Wei J., Li W., Yue F., Song Y., *et al.* 2021. Mechanisms underlying the effects of Lianhua Qingwen on sepsis-induced acute lung injury: a network pharmacology approach. Front Pharmacol. 12:717652. https://doi.org/10.3389/fphar.2021.717652

Yang Y., Zhong Z.T., Xiao Y.G. and Chen H.B. 2022. The activation of AMPK/NRF2 pathway in lung epithelial cells is involved in the protective effects of kinsenoside on lipopolysaccharide-induced acute lung injury. Oxid Med Cell Longev. 2022:3589277. https://doi.org/10.1155/2022/3589277

Yimam M., Horm T., O'Neal A., Jiao P., Hong M. and Jia Q. 2023. UP360, a standardized composition from extracts of Aloe barbadense, Poria cocos, and Rosemary officinalis protected against sepsis and mitigated acute lung injury in murine models. J Med Food. 26(7):489–499. https://doi.org/10.1089/jmf.2022.0136

Zeng M., Sang W., Chen S., Chen R., Zhang H., Xue F., *et al.* 2017. 4-PBA inhibits LPS-induced inflammation through regulating ER stress and autophagy in acute lung injury models. Toxicol Lett. 271:26–37. https://doi.org/10.1016/j.toxlet.2017.02.023

Zeng T., Zhou Y., Yu Y., Wang J.W., Wu Y., Wang X., *et al.* 2023. rmMANF prevents sepsis-associated lung injury via inhibiting endoplasmic reticulum stress-induced ferroptosis in mice. Int Immunopharmacol. 114:109608. https://doi.org/10.1016/j.intimp.2022.109608

Zhai F.G., Liang Q.C., Wu Y.Y., Liu J.Q. and Liu J.W. 2022. Red ginseng polysaccharide exhibits anticancer activity through GPX4 downregulation-induced ferroptosis. Pharm Biol. 60(1):909–914. https://doi.org/10.1080/13880209.2022.2066139

Zhang M.Q. and Li C.S. 2023. Therapeutic effects of Shenfu injection in shock. Chin J Integr Med. 29(12):1142–1146. https://doi.org/10.1007/s11655-023-3631-2

Zheng G., Ren H., Li H., Li X., Dong T., Xu S., *et al.* 2019. Lycium barbarum polysaccharide reduces hyperoxic acute lung injury in mice through Nrf2 pathway. Biomed Pharmacother. 111:733–739. https://doi.org/10.1016/j.biopha.2018.12.073

Zhou X. and Liao Y. 2021. Gut-lung crosstalk in sepsis-induced acute lung injury. Front Microbiol. 12:779620. https://doi.org/10.3389/fmicb.2021.779620

Zhou J., Peng Z. and Wang J. 2021. Trelagliptin alleviates lipopolysaccharide (LPS)-induced inflammation and oxidative stress in acute lung injury mice. Inflammation. 44(4):1507–1517. https://doi.org/10.1007/s10753-021-01435-w